PROCEEDINGS, 49th Workshop on Geothermal Reservoir Engineering
Stanford University, Stanford, California, February 12-14, 2024
SGP-TR-227

Characterizing Structure in Southern Summer Lake Valley, Oregon Using Ground- and sUAS-Based Potential Field Geophysics

Tait E. Earney and Jonathan M. G. Glen

U.S. Geological Survey, 350 N. Akron Road, Building 19, Moffett Field, CA 94035

tearney@usgs.gov

Keywords: Summer Lake, geophysics, potential fields, gravity, magnetics, paleomagnetics, rock properties, sUAS

ABSTRACT

Summer Lake is located in south-central Oregon at the extreme northwestern extent of the Basin and Range Province, bordered by the Cascade Volcanic Province to the west and the High Lava Plains to the north. The valley hosts numerous hot springs and a small geothermal powerplant at the southeastern end of the valley in the town of Paisley. This tectonically active region has undergone significant ENE-directed extension producing highly faulted terrain with fault blocks tilting on average 60° from the maximum extension direction. Local geology consists of young volcanics which have been extensively dissected by predominantly NNW-trending normal faults. These same structures likely extend through the basin but are concealed by young basin fill sediments and volcanics. As a result, potential field geophysical methods are ideally suited for characterizing subsurface geology and structures in this region which are important for understanding basin evolution and tectonics within the valley. New ground-based gravity and magnetic data, as well as sUAS- (small uncrewed aerial systems) based magnetic data reveal a prevalent NNW-trending fabric beneath the basin fill in southern Summer Lake valley that likely plays an important role in controlling the flow of subsurface hydrothermal fluids. Additionally, measurements were performed on outcrops, hand samples and paleomagnetic cores to constrain the physical properties (density, magnetic susceptibility and magnetic remanence) of local geology. Together, these data help resolve basin geometry and delineate concealed faults and contacts, informing our understanding of the structural framework and geothermal resource potential of southern Summer Lake valley.

1. INTRODUCTION

Summer Lake valley is located in a remote part of south-central Oregon and is situated between three distinct geologic and tectonic provinces. It lies within the northwest corner of the Basin and Range Province, a region of geothermal resource potential (Coolbaugh et al., 2002; Coolbaugh and Shevenell, 2004), along the eastern edge of the Cascade Volcanic Range, and along the southern border of the High Lava Plains (Figure 1). The area is characterized by regional EW to slightly NE-SW directed extension (Pezzopane and Weldon, 1993) that dissipates northward into the gentle warping of the High Lava Plains. Crustal thinning as a result of the extension is responsible for elevated heat flow in the region (Blackwell, 1983; Makovsky, 2013) and numerous hydrothermal springs.

Structural complexity is the driver of many hydrothermal systems, because they provide permeable pathways for fluid migration in the subsurface (Faulds and Hinz, 2015). Determining the structural controls of fluid flow in active hydrothermal systems requires a detailed understanding of subsurface geological features, including locations and geometries of faults and contacts, basin shape and depth, as well as locations of possible alteration zones. However, this information is inherently difficult to validate from surface observations alone. Drill holes can provide some of the most valuable subsurface data, but they are usually sparse, shallow, or non-existent in a given field area. Therefore, potential field geophysical methods can be extremely useful for characterizing the structural framework controlling a hydrothermal system.

The geology of the region consists of widespread basaltic and andesitic flows with interbedded, locally thick (few hundred meters) sections of tuff and tuffaceous lacustrine sediments (Beaulieu, 1972; Wells, 1975), creating an ideal environment for potential field geophysical studies due to the large contrast in physical properties between lithologies. Here, we will discuss our geophysical (gravity, magnetic) and rock property (density, magnetic susceptibility, magnetic remanence) data collection and how they are combined to characterize the structural framework of Summer Lake valley.

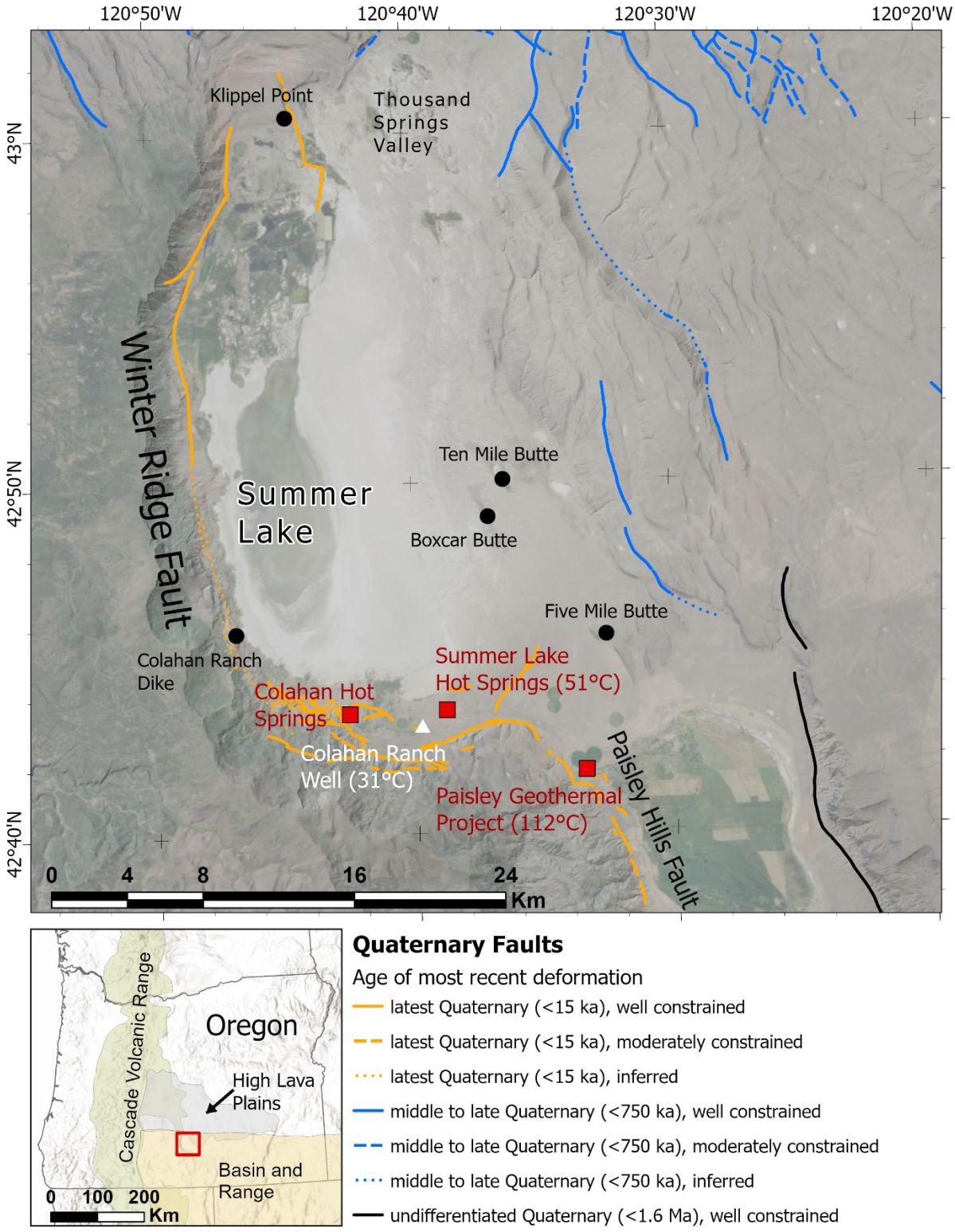

Figure 1: Map of the study area displaying a 10-meter digital elevation model (DEM) hillshade (U.S. Geological Survey, 2022) overlain by aerial imagery (Esri, 2023). Quaternary faults (U.S. Geological Survey, 2022) are represented by the colored lines with the color and line type corresponding to the age of the fault and confidence in its location, respectively. Also displayed are three zones of thermal upwelling at Colahan Hot Springs, Summer Lake Hot Springs (temperature from Black, 1994), and the Paisley Geothermal Project (temperature from Williams et al., 2016). The inset map shows a topographic hillshade (Esri, 2023) overlain by the location of the study area (red polygon) in relation to major geologic and tectonic terranes (Basin and Range extent – DeAngelo et al., 2022; Cascades Volcanic Range extent – Priest, 1990; High Lava Plains extent – Meigs et al., 2009).

2. METHODS

Potential field geophysical methods are valuable tools for characterizing subsurface geology and structure as they facilitate identification of features which may be concealed by overlying basin fill sediments. Natural variations in gravity and magnetic fields arise from lateral and vertical contrasts in rock density and magnetic properties. These contrasts can occur due to a number of factors (e.g., lateral facies changes within a single unit, hydrothermal alteration, offset across faults, or geological contacts with other rock units), and are responsible for producing the gravity and magnetic anomalies observed at the surface. With sufficient detailed, high-resolution data we can infer the shape, depth, and lateral extent of the buried source rocks, and characterize fault geometries and offsets. These methods are particularly useful in places such as Summer Lake valley, where the landscape is dominated by young basin fill sediments which overlie relatively dense and strongly magnetic volcanic rocks. From 2011 to 2022, we collected gravity, ground-based magnetic, rock property (density, magnetic susceptibility, magnetic remanence), and sUAS-based magnetic data throughout Summer Lake valley to investigate structural controls on basin development and hydrothermal activity in the region.

2.1 Gravity

The existing gravity data coverage in Summer Lake valley was quite sparse prior to our study. Legacy data included 464 gravity stations spanning an area of ~80x90 km around the study area, which were extracted from a public domain dataset (Hildenbrand et al., 2002; database was made available from University of Texas, El Paso on 5/29/2018 [Ben Drenth, written commun., 3/11/2021]), and 170 gravity stations spanning the north end of Summer Lake valley (Travis, 1977). These data were re-reduced so they could be merged with the new data acquired between 2011 and 2022. We collected 882 new gravity stations along detailed profiles across local focus areas in the southeast portion of the basin near the Paisley Geothermal Project, Summer Lake Hot Springs and a topographic feature on the east side of the basin herein referred to as Boxcar Butte (Figure 2A), and also focused on filling in data gaps between existing stations to improve the regional coverage.

New and existing gravity data were reduced using standard gravity reduction methods (Blakely, 1995), with an assumed average crustal density of 2,670 kg/m^3, and included the following corrections: 1) Earth-tide corrections, which account for tidal effects from the moon and sun; 2) instrument drift correction, which compensates for the linear drift of the gravity meter's spring; 3) latitude correction, which corrects for the variation in the gravity field relative to latitude; 4) free-air correction, which accounts for the effect of the elevation of the gravity measurement relative to sea level; 5) Bouguer correction, which corrects for the gravitational attraction of material between the location of the measurement and sea level; 6) curvature correction, which adjusts the Bouguer correction to account for the curvature of the Earth's surface; 7) terrain correction, which removes the effect of the gravitational attraction of topography within a radial distance of 167 kilometers from each measurement location; and 8) isostatic correction, which accounts for long-wavelength variations in the gravity field caused by deep masses that isostatically support topographic loads. Terrain corrections were calculated using a combination of manual and digital methods. In most areas of Earth's surface (including our study area), the highest resolution digital elevation models (DEMs) have a resolution of 10 meters, which are typically not sufficient to accurately characterize any extreme changes in topography that locally distort the gravitational field near any individual station location. Therefore, at each station location we calculated a field terrain correction manually. Field terrain corrections were calculated for a radial distance extending 68 meters from the station location by simplifying the terrain into uniform slopes and calculating their gravitational influence using established charts (Hayford and Bowie, 1912). Beyond 68 meters from the station, the gravitational influence of topography is less, such that 10- and 30-meter DEMs are sufficient to calculate the remaining terrain correction.

After reducing and merging the gravity data, we used the minimum curvature gridding routine available in Oasis Montaj® geophysical modeling and analysis software (Seequent, 2022) to produce an updated isostatic anomaly map for Summer Lake valley and adjacent areas with a grid cell size of 500 meters. Note that the grid cell size is limited by the sparsity of the regional data, however, higher-resolution 2D profiles can be extracted for modeling along detailed profiles where station spacing is much tighter. We then derived a residual isostatic anomaly map by analytically continuing the original isostatic anomaly map upwards 500 meters and subtracting the result from the original isostatic anomaly map (Figure 2B). The residual isostatic anomaly highlights subtle, shallow crustal features that might otherwise be difficult to recognize in the presence of regional fields, aiding structural mapping and interpretation of subtle, shallow-source anomalies.

Although the new gravity compilation provides detailed coverage across the local focus areas, the regional coverage is still sparse, particularly on the west side of the basin which is usually covered by water and wetlands, and in the High Lava Plains east of the basin where road access is extremely limited. As a result, care should be taken in interpreting gravity maps in these areas.

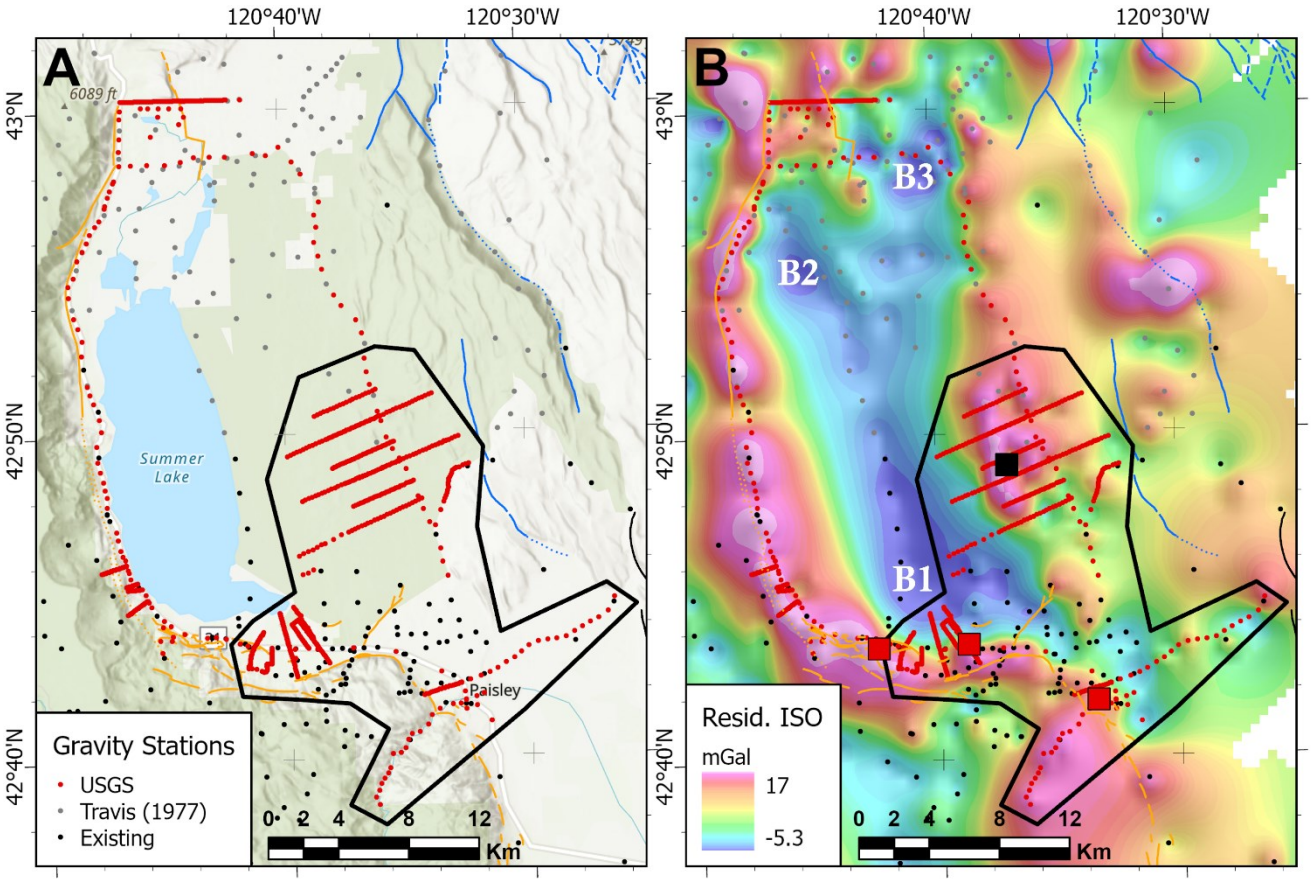

Figure 2: A) World topographic map (Esri, 2024) overlain by Quaternary faults (U.S. Geological Survey, 2022) and gravity station locations. The extent of Figure 10 is indicated by the black outline. B) Residual isostatic anomaly map overlain by Quaternary faults (U.S. Geological Survey, 2022), gravity station locations, and points representing the locations of Boxcar Butte (black square), Colahan Hot Springs, Summer Lake Hot Springs, and the Paisley Geothermal Project (red squares; left to right, respectively). Locations of sub-basins referenced in the discussion are denoted by B1, B2 and B3. The extent of Figure 10 is indicated by the black outline. Refer to Figure 1 for fault symbology description.

2.2 Magnetics

Existing aeromagnetic data (Roberts et al., 2008) over much of south-central Oregon is very coarse. In our study area, the Oregon state aeromagnetic compilation is characterized by line spacings of 2,400 meters, and a barometric flight altitude of 1,700 meters, which is unsuitable for quantitative analyses and robust geologic interpretation at the scale of our research. Just south of Summer Lake valley is a much higher resolution aeromagnetic/aeroradiometric survey (Hill et al., 2009; originally flown in 1979; herein referred to as Lakeview aeromagnetic survey), with primary survey lines flown east-west and spaced 400 meters apart, and a draped survey height of nominally 120 meters above topography (area A in Figure 3). There appeared to be uncorrected heading errors in the raw data for this survey, causing substantial corrugation of the data along flight lines. In the absence of any calibration information to compensate for this, we applied a directional cosine filter (available through the 2D Filtering extension of Oasis Montaj®) to the gridded raw data, to isolate and remove the corrugated signal along the azimuth of the flight lines (270°). The result was a much cleaner grid that could be used to map continuous structural features that had previously been unrecognizable in the unfiltered data. Although this survey does not extend over our primary area of interest for this study it does cover the Paisley Geothermal Project and Summer Lake Hot Springs, in addition to covering the apparent left-step between the Paisley Hills fault zone and the Winter Ridge fault zone, providing valuable context for interpreting structures and geology trending into the southern reaches of Summer Lake valley.

Due to the lack of regional high quality airborne magnetic data, and to better characterize subtle anomalies associated with concealed faults and geologic contacts, we collected ~253 line-kilometers of high-resolution ground-based magnetic data throughout Summer Lake valley (areas B, C, D, E, and F in Figure 3). The data were diurnally corrected, and anomalies associated with "cultural noise" (e.g., metal fences, buildings, power lines, culverts, passing vehicles, etc.) were removed. Following post-processing, the ground-based magnetic data collected in the region around Boxcar Butte (area B in Figure 3) and the filtered Lakeview aeromagnetic survey data were gridded using the minimum curvature routine in Oasis Montaj® to produce total field (TF) magnetic anomaly maps with grid cell sizes of 100 meters. The ground-based magnetic data collected in the other areas outlined on Figure 3 (areas C, D, E and F) are too sparse for grid interpolation. However, the profile data along individual transects do provide accurate locations of buried faults and contacts. Pseudogravity and reduced-to-pole (RTP) transformations (Blakely, 1995) were subsequently applied to the TF magnetic anomaly maps to simplify and center the anomalies over their sources. The pseudogravity transformation converts a magnetic anomaly into one that would be observed

if the magnetic distribution of the source material was replaced by an identical density distribution, assuming that more magnetic rocks are also likely more dense (than non-magnetic rocks). This transformation removes edge effects at the boundaries of magnetic anomalies, simplifying the analysis of their sources, and allowing a more direct comparison with gravity anomalies. The RTP transformation is a method that converts magnetic anomalies to those that would be observed if the ambient magnetic field were vertically oriented, which effectively centers magnetic anomalies over their source rocks. Both methods allow for simpler, more geologically reasonable structural interpretations. The RTP grids for both the Lakeview aeromagnetic survey and the ground-based magnetic survey over Boxcar Butte are shown in Figures 4 and 5 respectively.

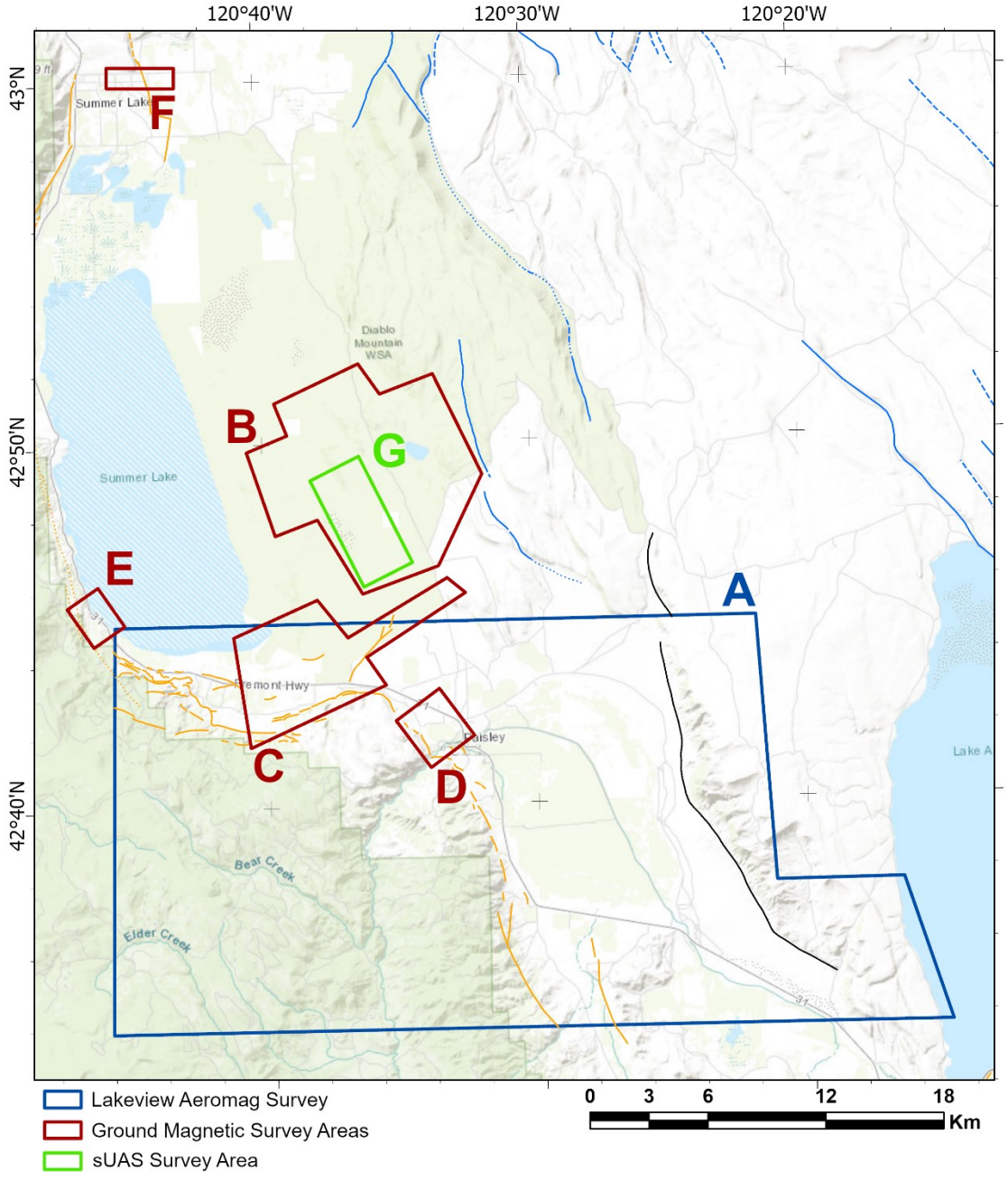

Figure 3: World topographic map (Esri, 2024) overlain by Quaternary faults (U.S. Geological Survey, 2022), Lakeview aeromagnetic survey extent (blue polygon; Hill et al., 2009), ground-based magnetic survey extents (red polygons), and the sUAS-based magnetic survey extent (green polygon). Colored letters are used as a reference for survey areas in subsequent figures. Refer to Figure 1 for fault symbology description.

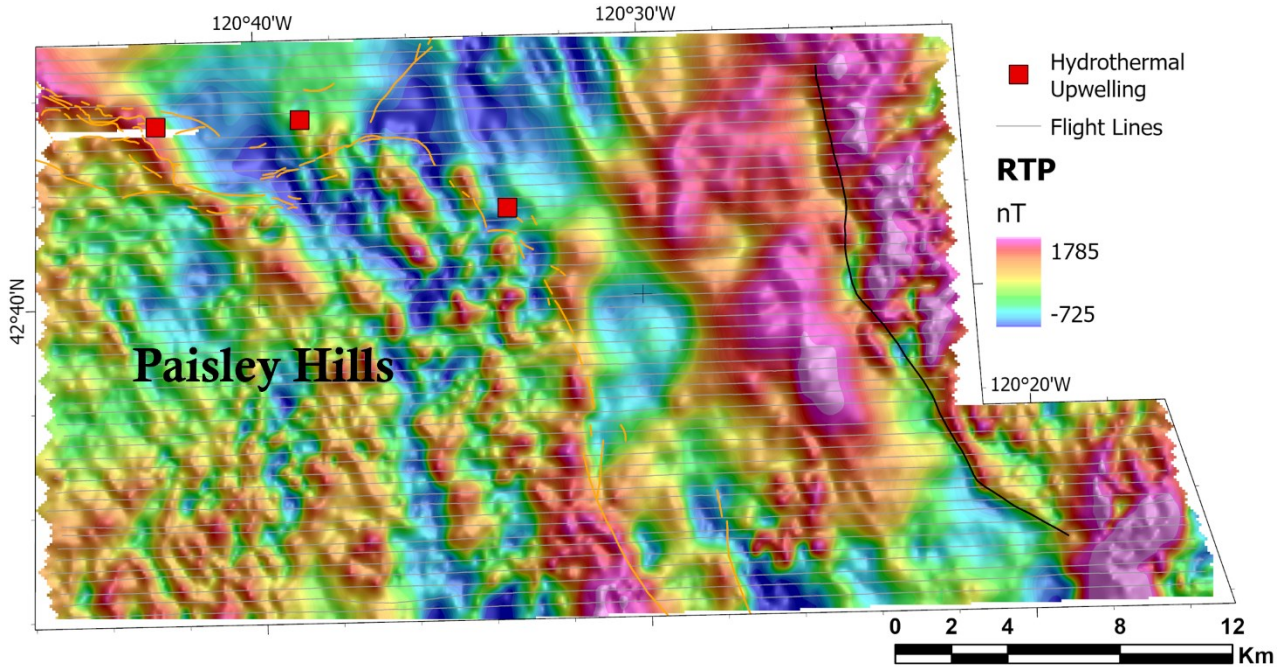

Figure 4: Shaded RTP magnetic anomaly map of the Lakeview aeromagnetic survey (area A on Figure 3; Hill et al., 2009). Also shown are the locations of hydrothermal upwelling at Colahan Hot Springs, Summer Lake Hot Springs, and the Paisley Geothermal Project (red squares; left to right, respectively), flight lines (grey lines), and Quaternary faults (U.S. Geological Survey, 2022). Refer to Figure 1 for fault symbology description.

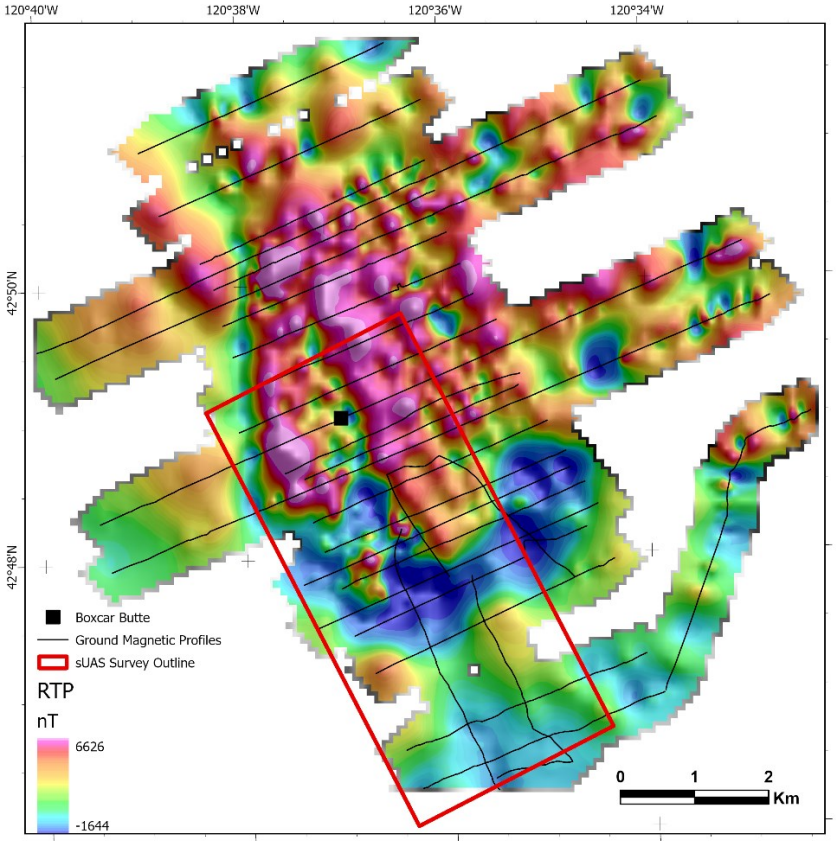

Figure 5: Shaded RTP magnetic anomaly map of the ground-based magnetic survey in the region around Boxcar Butte (area B on Figure 3) overlain by profile locations (black lines) and the location of Boxcar Butte (black square). The extent of the sUAS-based magnetic survey (Figures 9 and 13) is indicated by the red polygon.

2.3 Rock Properties

Rock property data provide necessary constraints to potential field models and are key to making informed geological interpretations of geophysical datasets. For this study, we collected density, magnetic susceptibility and paleomagnetic (magnetic remanence) data to constrain lithologies relevant to our geophysical mapping efforts. Where possible, samples and measurements were collected from fresh unaltered portions of an outcrop. See Figure 6 for rock property sampling locations.

Rock density information is crucial to understanding the sources of gravity anomalies. We measured the saturated bulk densities (SBD) of 36 hand-sized rock samples from 17 unique outcrop locations. In the Chewaucan River Canyon southwest of Paisley, we sampled both volcanic flows and mafic dikes from eight distinct units. At Boxcar Butte we collected samples at three different locations, but it was unclear whether the samples were from intrusive or extrusive units. Hand samples from Ten Mile Butte were collected from six separate volcanic flows and consisted mostly of vesicular lavas.

Constraining rock-magnetic properties (magnetic susceptibility and magnetic remanence) is essential to modeling and interpreting sources of anomalies in settings like Summer Lake valley that host strongly magnetic mafic volcanic rocks. A total of 446 magnetic susceptibility measurements were made on hand samples and outcrops using a ZH Instruments SM30 susceptibility meter, including three measurements on each of the 36 hand samples that were collected, and 334 at 28 unique outcrop locations. An average of 12 susceptibility measurements were performed on each outcrop with measurements spread out over several meters to capture any lateral variations in magnetic susceptibility that can occur within lithologic units (e.g., lateral facies changes, hydrothermal alteration, surface weathering, etc.). Additional outcrop susceptibilities were also measured on a mafic dike on Colahan Ranch, as well as on three stacked flows at Klippel Point. See Table 1 and Figure 7 for a summary of hand sample densities and outcrop susceptibilities.

Crustal magnetic fields depend on both the induced and remanent magnetizations of underlying rocks. In many cases, magnetic remanence is ignored because either the magnitude is negligible, or the direction is close to the induced field direction. However, in strongly magnetic rocks, such as the mafic lavas and intrusions found in and around Summer Lake valley, the remanent component can be quite substantial and must be considered. To characterize the remanent magnetization properties of local volcanic rocks in Summer Lake valley, we collected oriented paleomagnetic cores from 45 unique sites, sampling both lava flows and intrusive bodies. Typically, six to eight cores were required at each site in order to confidently constrain the remanent direction, however, the final number of cores collected at each site was dependent on the accessibility and quality (e.g., degree of weathering, presence of lightning strikes, etc.) of the outcrop. Magnetic remanence measurements were performed on a total of 290 individual paleomagnetic cores. Sample data were fit using principal component analysis to determine characteristic remanent magnetization (ChRM) directions (Kirschvink, 1980) and great circle analyses to determine great circle trends (McFadden and McElhinny, 1988). Site mean paleomagnetic directions and confidence circles (Figure 8) were calculated using modified Fisher statistics (Fisher, 1953).

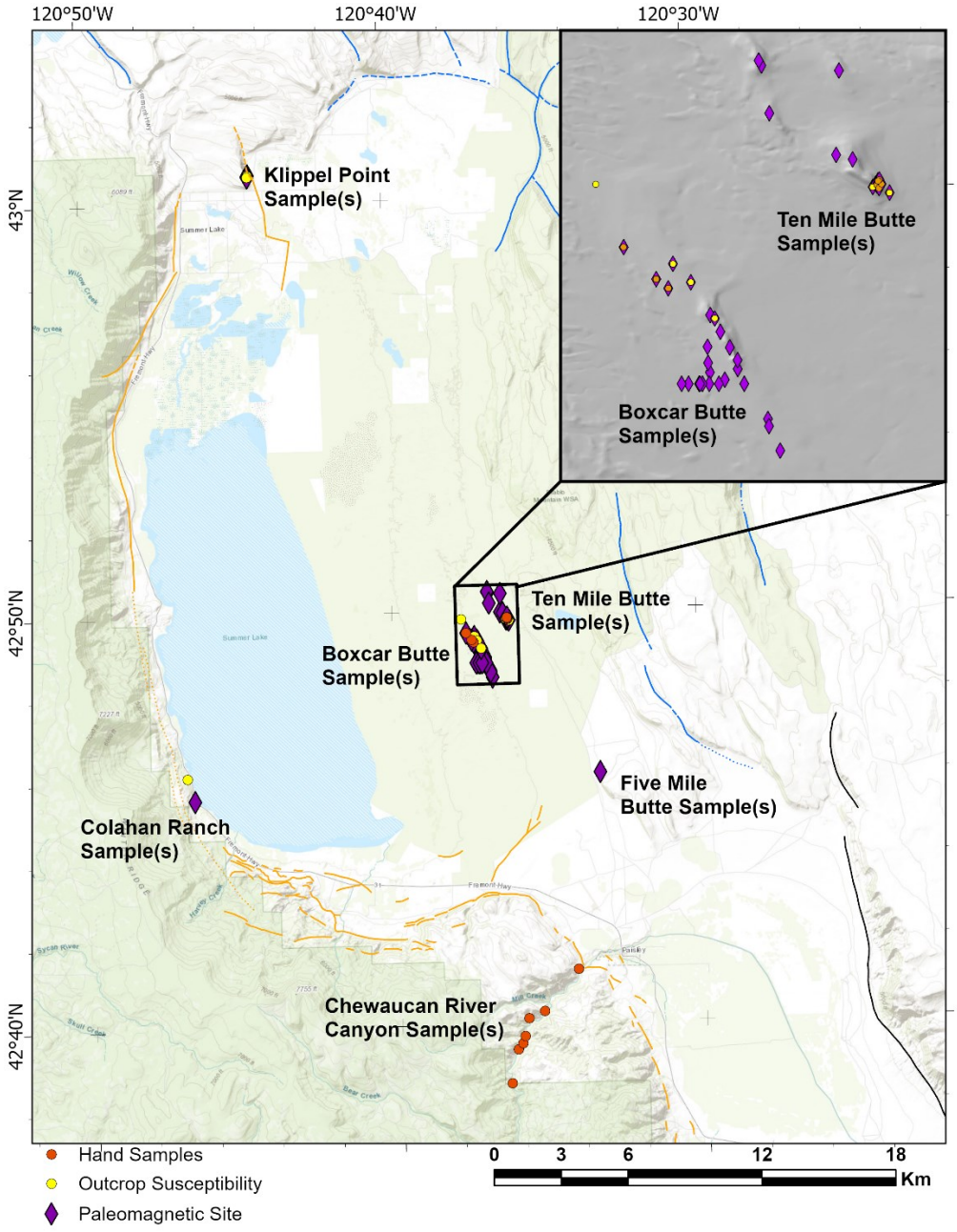

Figure 6: World topographic map (Esri, 2024) overlain by Quaternary faults (U.S. Geological Survey, 2022), hand-sample sites (orange dots), outcrop susceptibility sites (yellow dots), and paleomagnetic sites (purple diamonds). Refer to Figure 1 for fault symbology description. Base map for inset figure is a 10-meter DEM hillshade (U.S. Geological Survey, 2022).

Table 1: Summary of average hand sample densities and outcrop susceptibilities according to the geographic region they were collected in and the rock type they represent.

Location	Rock Type	SBD (kg/m^3)	Susceptibility (x10^{-3})
Boxcar Butte	Dikes/Lavas?	2,917	44.2
Chewaucan River Canyon	Dikes	2,489	16.0
Chewaucan River Canyon	Lavas	2,711	29.3
Colahan Ranch	Dikes	NA	15.4
Klippel Point	Lavas	NA	12.3
Ten Mile Butte	Lavas	2,812	16.7

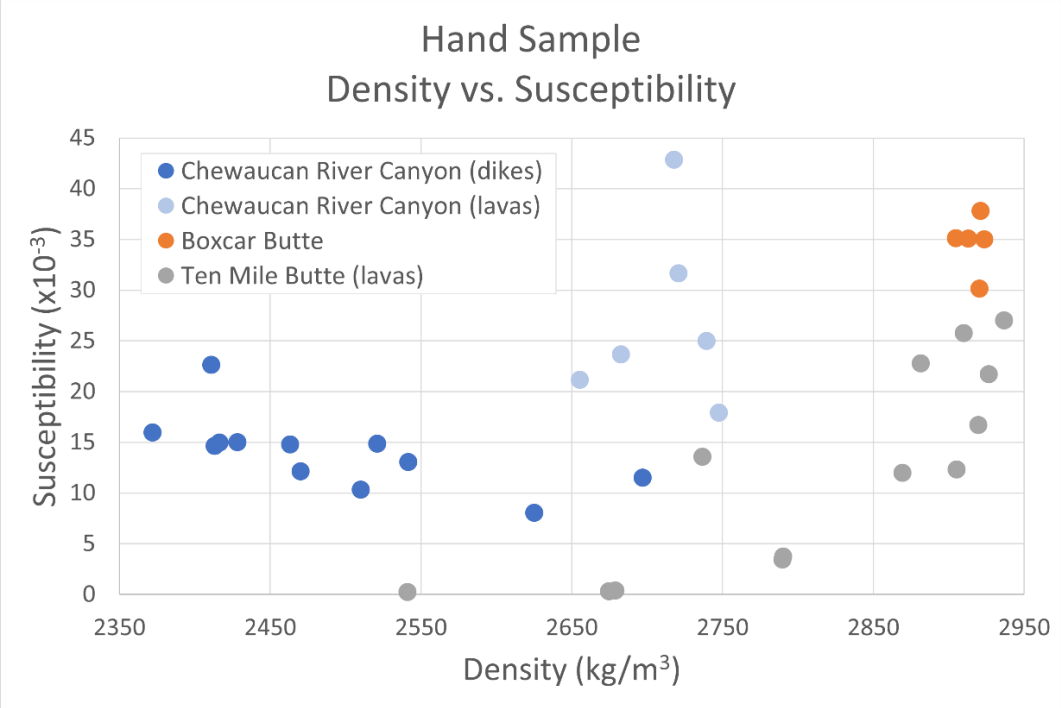

Figure 7: Scatter plot displaying the densities (x-axis) and susceptibilities (y-axis) of hand samples. Dark and light blue dots correspond to samples from dikes and lavas, respectively, in the Chewaucan River Canyon, orange dots correspond to samples from Boxcar Butte that may be dikes and/or lavas, and grey dots correspond to samples from lavas at Ten Mile Butte.

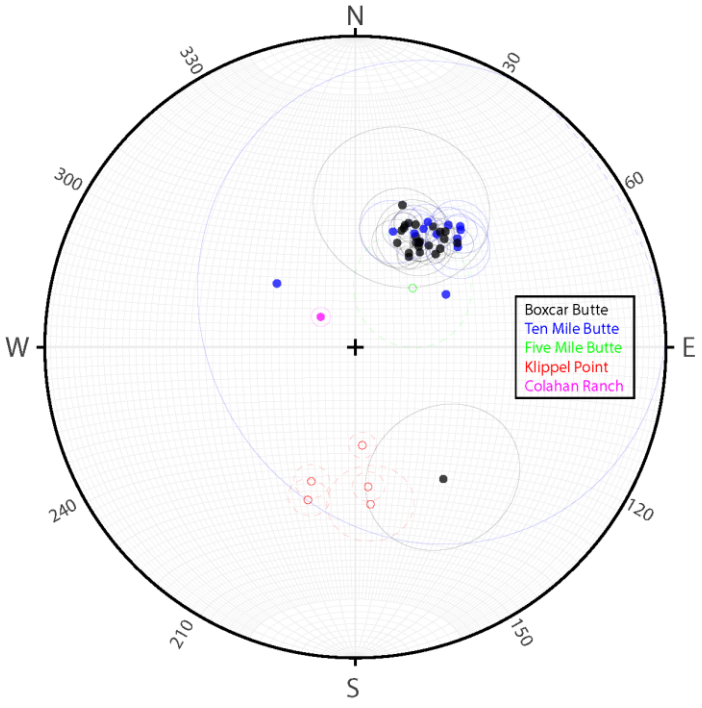

Figure 8: Stereoplot of paleomagnetic site best-fit directions colored by location where samples were collected. Directions and alpha 95 confidence circles corresponding with normal polarity magnetizations (lower hemisphere) are depicted by closed symbols and solid circles, respectively. Directions and alpha 95 confidence circles corresponding with reversed polarity magnetizations (upper hemisphere) are depicted by open symbols and dashed circles, respectively.

2.4 sUAS Magnetics

Recent advances in the development of sUAS for geophysical data acquisition has substantially improved the rate at which geophysical data can be collected compared to ground-based survey methods, in addition to providing higher quality, more spatially continuous datasets (Kaub et al., 2021; Rea-Downing et al., 2023). For this study, we deployed a DJI Matrice 600 Pro to collect sUAS-borne magnetic data over Boxcar Butte on the east side of Summer Lake valley. We collected 81.7 line-kilometers of sUAS-borne magnetic data. The survey was draped over topography with a nominal flight height of 120 meters above ground level. Primary survey lines were along an azimuth of 245° and were spaced 240 meters apart. Tie lines were flown perpendicular to the survey lines along an azimuth of 155° and were spaced 370 meters apart. The data were processed using the publicly available MagComPy software (Kaub et al., 2021) which applies a diurnal correction, compensates for magnetic perturbations that originate from the aircraft (e.g. heading errors), and computes cross over differences between intersecting survey lines to assess the quality of the compensation. Following post processing, the same procedures outlined for the ground-based magnetic and existing aeromagnetic data (section 2.2) were followed to produce TF, RTP (Figure 9), and pseudogravity magnetic anomaly maps for the sUAS magnetic data using a grid cell size of 100 meters.

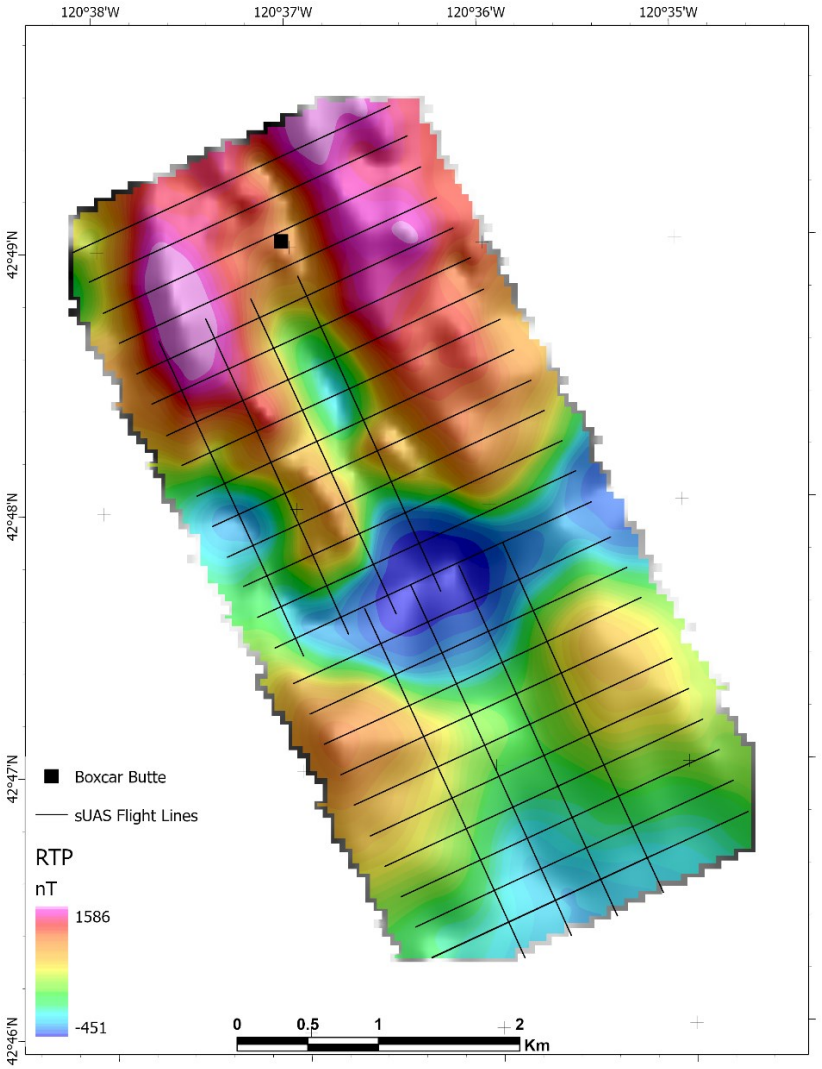

Figure 9: Shaded RTP magnetic anomaly map (area G on Figure 3) for the sUAS-based magnetic data. Flight line locations are indicated by the black lines and the location of Boxcar Butte is indicated by the black square.

3. STRUCTURAL MAPPING

We employed various derivative and filtering methods to extract structural information from the gravity and magnetic maps that can be used to delineate the lateral extent of concealed faults and contacts. Subsurface structures typically manifest as steep gradients in potential field data and can be mapped by analyzing the horizontal gradient maxima (HGM; Blakely and Simpson, 1986) of gravity and pseudogravity anomalies. This method assumes that HGM tend to lie over near-vertical edges of potential field sources. In reality, many structures will have a dip component, causing the mapped location of their corresponding HGM to be shifted in the direction of dip (Cordell and Grauch, 1982). Constraints on the HGM, as well as any geophysically-derived interpretations, depend on the underlying data distribution. In general, the regional gravity data coverage in Summer Lake valley is too widely spaced to infer any meaningful structural

interpretations from the HGM beyond the regions around Boxcar Butte, Summer Lake Hot Springs and the Paisley Geothermal Project where there is sufficient data density to provide constraints on the locations and trends of the HGM. For magnetics, only the ground and sUAS-based magnetic surveys at Boxcar Butte and the Lakeview aeromagnetic survey are sufficient to rely on the HGM for structural interpretations.

In Oasis Montaj®, we produced horizontal gradient (HG) maps of both the isostatic gravity and pseudogravity anomalies. Following Phillips et al. (2007) we calculated the HGM using a routine that identifies laterally continuous ridges in the HG maps. Discrete maxima were then connected into lines (or lineations) using a process that automates lineament detection in HGM point data based on user specified distance and azimuth relationships to adjacent maxima (Athens, 2018). See Figures 10, 11, 12 and 13 for lineations produced from the geophysical data.

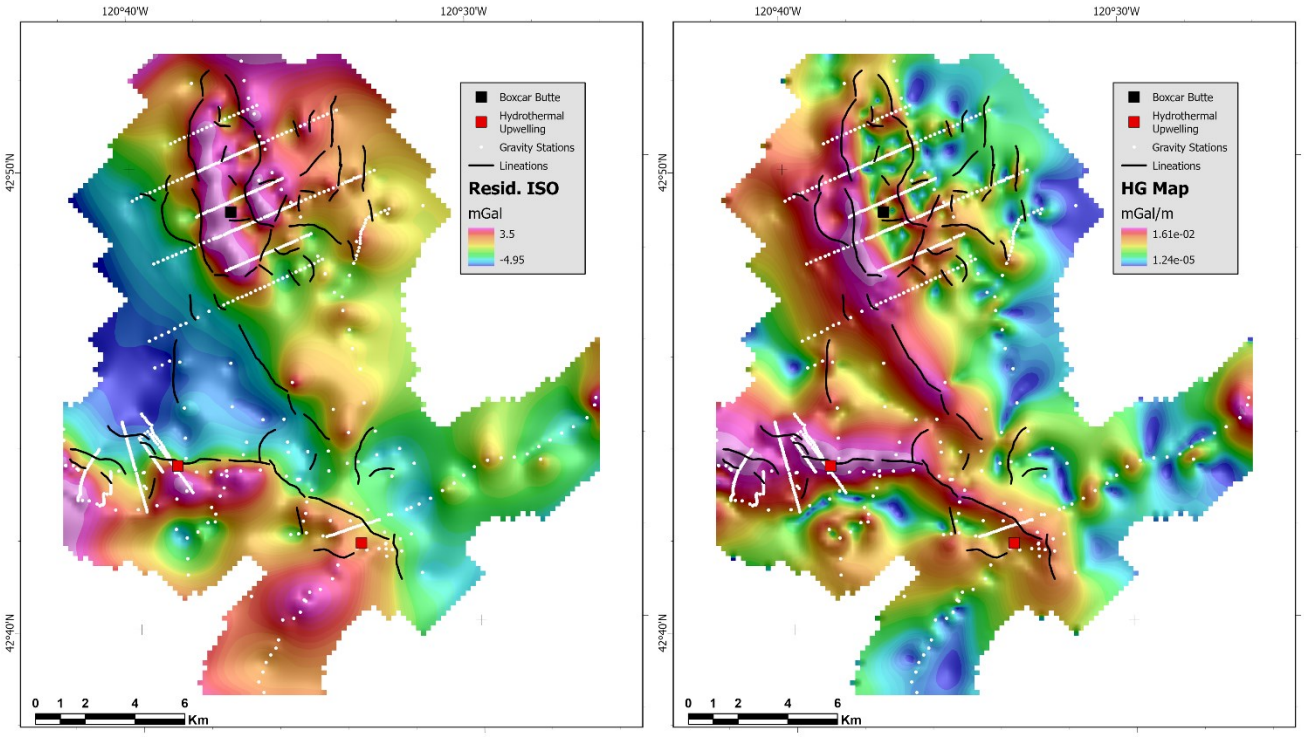

Figure 10: Left) Shaded residual isostatic gravity anomaly map. Right) Shaded HG map of the isostatic gravity anomaly. Both maps are overlain by lineations derived from the HGM (black lines), gravity station locations (white dots), and symbols indicating the locations of Boxcar Butte (black square) and zones of hydrothermal upwelling at Summer Lake Hot Springs and the Paisley Geothermal Project (red squares; left to right, respectively).

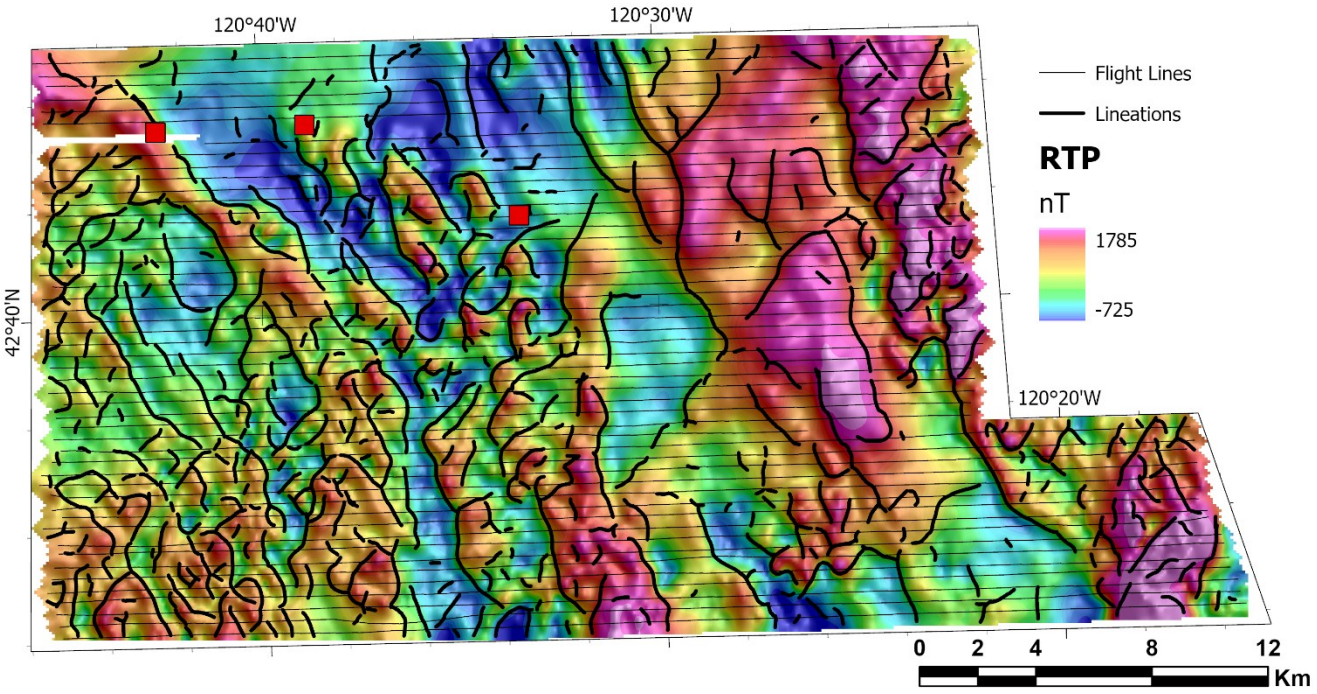

Figure 11: Shaded RTP magnetic anomaly map of the Lakeview aeromagnetic survey (area A on Figure 3; Hill et al., 2009) overlain by lineations derived from the HGM (black lines), flight lines (grey lines) and locations of hydrothermal upwelling at Colahan Hot Springs, Summer Lake Hot Springs and the Paisley Geothermal Project (red squares; left to right, respectively).

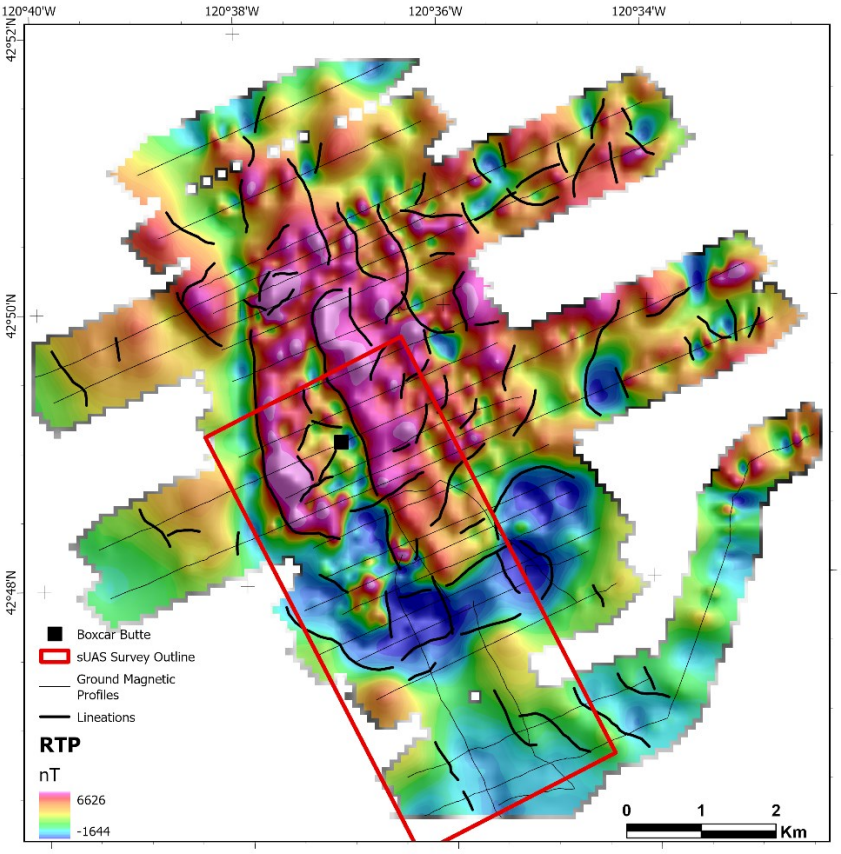

Figure 12: Shaded RTP magnetic anomaly map of the ground-based magnetic survey at Boxcar Butte (area B on Figure 3) overlain by lineations derived from the HGM (black lines), magnetic profile locations (grey lines) and the location of Boxcar Butte (black square). The extent of the sUAS-based magnetic survey (Figures 9 and 13) is indicated by the red polygon.

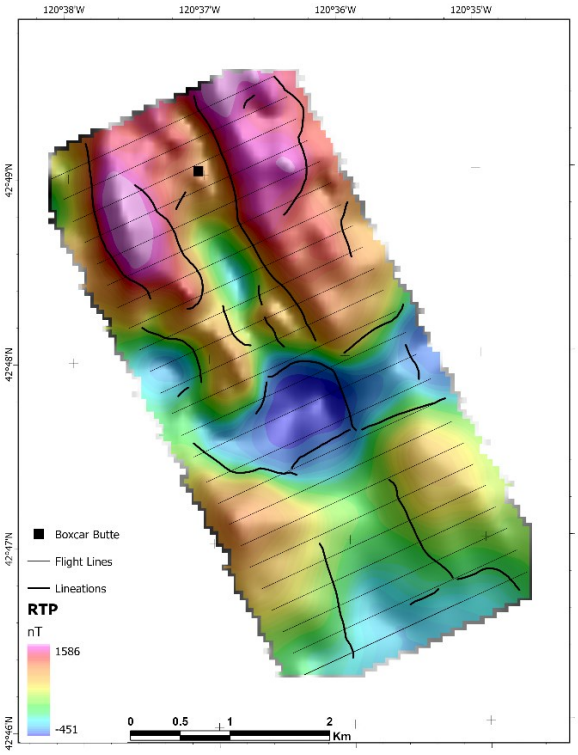

Figure 13: Shaded RTP magnetic anomaly map of the sUAS-based magnetic survey at Boxcar Butte (area G on Figure 3) overlain by lineations derived from the HGM (black lines), flight lines (grey lines) and the location of Boxcar Butte (black square).

Structural trends at the northern end of Summer Lake valley were previously defined by Travis (1977), who found that most faults, mapped at the surface, trend about N30°W, with relatively few faults trending either N-S or N20°E. Using faults sampled from the U.S. Geological Survey Quaternary fault database (U.S. Geological Survey, 2022) and the new geophysical lineations, we produced rose diagrams (Figure 14) to characterize structural trends in the southern half of Summer Lake valley. By incorporating geophysical lineations in the structural analysis, we account for concealed intra-basinal structural features, many of which have no surface manifestations, but may otherwise be important to controlling hydrothermal fluid flow within the basin.

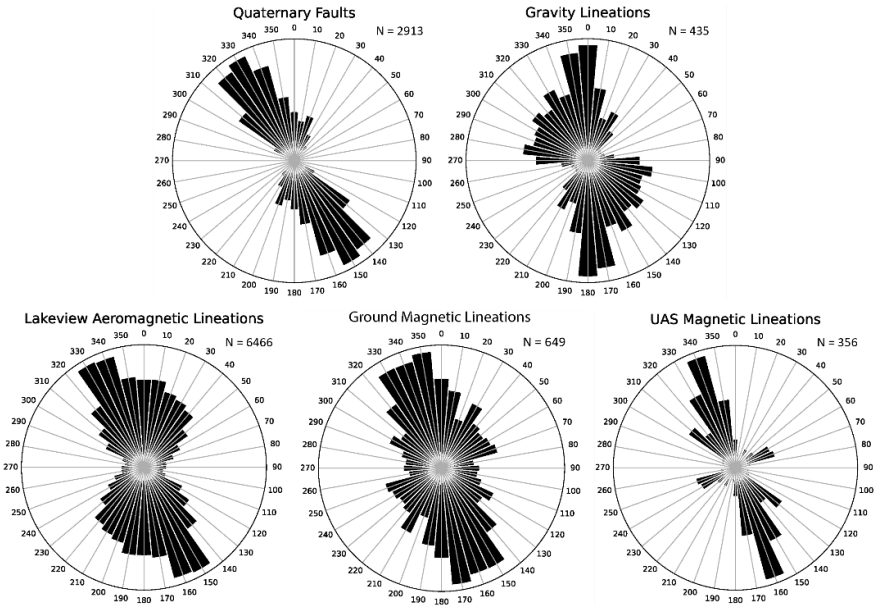

Figure 14: Rose diagrams for Quaternary faults (top left), gravity lineations (top right), Lakeview aeromagnetic lineations (bottom left), ground-based magnetic lineations (bottom center), and sUAS magnetic lineations (bottom right). N is the number of features used in the analysis.

4. DISCUSSION

The geophysical data collected for this study were used to resolve subsurface structures that have little or no surface manifestation. This is an essential step toward identifying potential pathways for hydrothermal flow. The study area occupies a region of substantial structural complexity because it is situated between three major geological/tectonic provinces: the Basin and Range Province to the south and southeast, the Cascade Volcanic Range to the west, and the High Lava Plains to the north (see Figure 1 index map). The complex geologic history of this region, and the fact that the entire area is either covered by basin fill sediments or volcanic rocks makes the geophysical methods employed here ideally suited for structural characterization.

The regional gravity data reveal a prominent, elongate gravity low that trends about N15°W, and is displaced towards the Winter Ridge range front on the west side of the basin, as previously suggested by Travis (1977). The lack of a large range front structure on the east side of the basin (like Winter Ridge on the west side), and the general trend of gravity values decreasing from east to west, lead us to conclude that Summer Lake valley is a structurally controlled, west-dipping asymmetric basin. Based on the gravity data they had at the time, Travis (1977) could distinguish two distinct sub-basins beneath the valley floor. With the new data collected as part of this study and modern gravity reduction and processing techniques, we believe there are at least three sub-basins apparent in the residual isostatic anomaly map; two smaller basins at the north end of the valley (B2 and B3 on Figure 2), and a larger, presumably deeper basin at the southern end of the valley (B3 on Figure 2). Another notable feature observed in the residual isostatic anomaly map is a N10°W trending, roughly 8.5-kilometer long and 4.5-kilometer wide intra-basin gravity high associated with outcrops of mafic volcanics in the vicinity of Boxcar Butte and Ten Mile Butte. The surface outcrops are much smaller than the gravity anomaly itself, suggesting the units are much more extensive at depth. The gravity HG map (Figure 10) shows a prominent, NNW-elongate high that begins just north of Boxcar Butte and trends southeast for nearly 15 kilometers. At its southern extent, it is nearly in line with the trend of the Paisley Hills Fault zone, and terminates near the Paisley Geothermal Project, which itself lies on the southern edge of a prominent NW trending gravity gradient at the intersection between the NNW-trending Paisley Fault zone and an EW-trending fault zone. This suggests that subsurface NNW-trending structures associated with the Paisley Hills Fault zone may extend well north of their currently mapped extents.

The Lakeview aeromagnetic survey provides high resolution coverage over the southern end of Summer Lake valley, including Summer Lake Hot Springs and the Paisley Geothermal Project, as well as the step-over between the Paisley Fault zone and the Winter Ridge Fault zone. Along the northern extent of the survey, several discreet NNW-trending linear features are observed where there are no faults mapped at the surface. Similar trends are also observed in the ground- and sUAS-based magnetic anomalies at Boxcar Butte. The trends of these features are nearly identical to the trend of the Paisley Hills Fault zone and other Quaternary faults observed east of the basin in the High Lava Plains, suggesting that they extend well into the subsurface beneath the southern reaches of Summer Lake valley.

Trends of both gravity and magnetic lineations agree very well with regional fault patterns (Figures 10, 11, 12 and 13). Quaternary faults within the region surrounding the study area trend about N30°W, whereas combined ground- and sUAS-based magnetic lineations trend N25°W, and gravity lineations, where data density is sufficient to allow quantitative analysis, trend about N10°W.

One of the key focuses of this study was investigating Boxcar Butte and its potential relationship to geothermal resources in the basin. The topographic expression of Boxcar Butte is around 700 meters long, 100 meters wide, and about 30 meters higher than the surrounding topography; a very prominent landmark in an otherwise flat landscape. Regional geological mapping (Travis, 1977; Diggles, 1990) describes the lithology composing Boxcar Butte as basalt and does not distinguish it from other basaltic and andesitic volcanic flows to the east, suggesting an extrusive origin. Our observations of the outcrop have found no evidence of vessicularity, flow boundaries, rubble or oxidation zones typical of volcanic flows in the area. Individual volcanic flows in this part of south-central Oregon are typically only several meters thick (Walker, 1963; Walker et al., 1967; Peterson and McIntyre, 1970), making it unlikely that there would be no evidence of extrusive volcanic features along an outcrop of this size. The trend of Boxcar Butte is N25°W, nearly identical to Quaternary fault trends in the region which converge about N30°W (Figure 14). As such, we do not preclude the possibility that this feature is a manifestation of complex fault interactions with the layered extrusive volcanic stratigraphy on the east side of the basin, but its geometry and outcrop textures (or lack thereof) lead us to posit that Boxcar Butte could be a mafic dike. This conclusion has meaningful implications for the history of basin development and regional magmatism, which warrants more study. Boxcar Butte also coincides with the northward extension of major structures that control the Paisley Hills Fault zone and Paisley Geothermal Project, which can inform future studies of geothermal prospectivity in southern Summer Lake valley.

ACKNOWLEDGMENTS

We would like to thank Grant Rea-Downing and Jacob Anderson for constructive reviews of this manuscript. We thank Claire Bouligand, Nick Davatzes, Andy Lamb, Rich Hamm, William Schermerhorn, Laurie Zielinski, Branden Dean, and Gordon Keller for their help in conducting field work. We thank Rich Hamm (University of Arkansas) again for conducting the sUAS surveys. We also thank Silvio Pezzopane for joining us in the field and sharing his knowledge of the local geology and structure of the region with us. We are grateful for many of the local landowners we have had the pleasure of interacting with and who have allowed us to access their property. This research was funded by the U.S. Geological Survey Energy Program Geothermal Resources Investigations Project. Any use of trade, firm, or product names is for descriptive purposes only and does not imply endorsement by the U.S. Government.

REFERENCES

Athens, N.: Maxspots curvature, software available at: https://github.com/nathens/maxspots_curvature, (2018).

Beaulieu, J.D.: Geologic formations of Eastern Oregon, Oregon Department of Geology and Mineral Industries Bulletin, 73, (1972), 80.

Black, G.L.: Low-Temperature geothermal database for Oregon, Oregon Department of Geology and Mineral Industries Open File Report, O-94-08, (1994), 178

Blackwell, D.: Heat flow in the Northern Basin and Range Province, Proceedings, Geothermal Resources Council Special Report, 13, (1983), 81-93.

Blakely, R.J.: Potential theory in gravity and magnetic applications, New York, Cambridge University Press, (1995), 441.

Blakely, R.J., and Simpson, R.W.: Approximating edges of source bodies from magnetic and gravity anomalies, Geophysics, 51, (1986), 1494–1498.

Coolbaugh, M.F., Taranik, J.V., Raines, G.L., Shevenell, L.A., Sawatzky, D.L., Minor, T.B., and Bedell, R.: A Geothermal GIS for Nevada: Defining regional controls and favorable exploration terrains for extensional geothermal systems, Proceedings, Geothermal Resources Council Transactions, Reno, NV, (2002), 485-490.

Coolbaugh, M.F., and Shevenell, L.A.: A Method for estimating undiscovered geothermal resources in Nevada and the Great Basin, Proceedings, Geothermal Resources Council Transactions, Reno, NV, (2004), 13-18.

Cordell, L., and Grauch, V.J.S.: Mapping basement magnetization zones from aeromagnetic data in the San Juan Basin, New Mexico, Society of Exploration Geophysicists Annual Meeting, (1985), 181-197.

Crider, J.: Oblique Slip and the geometry of normal fault linkage: mechanics and a case study from the Basin and Range in Oregon, Journal of Structural Geology, 23, (2001), 1997-2009.

DeAngelo, J., Burns, E.R., Gentry, E., Batir, J.F., Lindsey, C.R., Mordensky, S.P.: Heat flow maps and supporting data for the Great Basin, USA, U.S. Geological Survey Data Release, (2022), https://doi.org/10.5066/P9BZPVUC.

Diggles, M.F., Conrad, J.E., Soreghan, G.A.: Geologic map of the Diablo Mountain Wilderness Study Area, Oregon, US Geol. Surv. Misc. Field Stud. Map, MF2121, (1990).

ESRI: ArcGIS Pro, 3.1.3, (2023)

ESRI: USGS Imagery Only Basemap, 1:9028 scale, (2021)

ESRI: World Topographic Map, 1:4000 scale, (2024)

Faulds, J., and Hinz, N.H.: Favorable tectonic and structural settings of geothermal settings in the Great Basin Region, western USA: Proxies for discovering blind geothermal systems, Proceedings, World Geothermal Congress, Melbourne, Australia, (2015), 6.

Fisher, R.: Dispersion on a sphere, Proceedings of the Royal Society of London, 217, (1953), 295-305, doi: 10.1098/rspa.1953.0064.

Geometrics, MagMap, 5.04, (2017).

Hildenbrand, T., Briesacher, A., Flanagan, G., Hinze, W., Hittleman, A., Keller, G., Kucks, R., Plouff, D., Roest, W., Seeley, J., Smith, D., and Webring, M.: Rationale and operational plan to upgrade the U.S. gravity database, U.S. Geological Survey Open File Report, OF 2002-463, (2002), doi: 10.3133/ofr02463.

Hill, P.L., Kucks, R.P., and Ravat, D.: Aeromagnetic and aeroradiometric data for the conterminous United States and Alaska from the National Uranium Resources Evaluation (NURE) Program of the U.S. Department of Energy: U.S. Geological Survey Open File Report, (2009), OF 2009–1129.

Kaub, L., Keller, G., Bouligand, C., Glen, J.M.G.: Magnetic surveys with unmanned aerial systems: Software for assessing and comparing the accuracy of different sensor systems, suspension designs and compensation methods, American Geophysical Union Annual Meeting, Geochemistry, Geophysics, Geosystems, 22, (2021), doi: 10.1029/2021GC009745.

Kirschvink, J.L.: The least-squares line and plane and the analysis of paleomagnetic data, Geophysical Journal International, 62, (1980), 699-718, doi: 10.1111/j.1365-246X.1980.tb02601.x.

Kirschvink, J.L., Kopp, R.E., Raub, T.D., Baumgartner, C.T., and Holt, J.W.: Rapid, precise, and high-sensitivity acquisition of paleomagnetic and rock-magnetic data: Development of a low-noise automatic sample changing system for superconducting rock magnetometers, American Geophysical Union Annual Meeting, Geochemistry, Geophysics, Geosystems, 9, (2008), doi:10.1029/2007GC001856.

Lurcock, P.C. and Wilson, G.S.: PuffinPlot: A versatile, user-friendly program for paleomagnetic analysis, American Geophysical Union Annual Meeting, Geochemistry, Geophysics, Geosystems, 13, (2012), doi:10.1029/2012GC004098.

Makovsky, K.: The geothermal system Near Paisley, Oregon: A tectonomagmatic framework for understanding the geothermal resource potential of southeastern Oregon, Masters Thesis, Boise State University, Boise, Idaho, (2013), 203.

McFadden, P.L., and McElhinny, M.W.: The combined analysis of remagnetization circles and direct observations in paleomagnetism, Earth and Planetary Science Letters, 87, (1988), 161-172, doi: http://dx.doi.org/10.1016/0012-821X(88)90072-6.

Meigs, A., Scarberry, K., Grunder, A., Carlson, R., Ford, M.T., Fouch, M., Grove, T., Hart, W.K., Iademarco, M., Jordan, B., Milliard, J., Streck, M.J., Trench, D., and Weldon, R.: Geological and geophysical perspectives on the magmatic and tectonic development, High Lava Plains and Northwest Basin and Range, in O'Connor, J.E., Dorsey, R.J., and Madin, I.P., Volcanoes to Vineyards: Geologic

field trips through the dynamic landscape of the Pacific Northwest, Geological Society of America Field Guide, 15, (2009), 435–470.

Ortolano, G., D'Agostino, A., Pagano, M., Visalli, R., Zucali, M., Fazio, E., Alsop, G., and Cirrincione, R.: ArcStereoNet: A new ArcGIS® toolbox for projection and analysis of meso- and micro-structural data, ISPRS International Journal of Geo-Information, 10, (2021), doi:10.3390/ijgi10020050

Peterson, N.V., and McIntyre, J.R., Reconnaissance geology and mineral resources of easter Klamath County and western Lake County, Oregon, Oregon Department of Geology and Mineral Industries, Bulletin 66, (1970), 70.

Pezzopane, S., and Weldon, R.J.: Tectonic role of active faulting in central Oregon, Tectonics, 12, (1993), 1140-1169.

Phillips, J.D., Hansen, R.O., and Blakely, R.J.: The use of curvature in potential-field interpretation, Exploration Geophysics, 38, (2007), 111-119.

Priest, G.R.: Volcanic and tectonic evolution of the Cascade Volcanic Arc, central Oregon, Journal of Geophysical Research, 95, (1990), 19, 583-19, 599.

Rea-Downing, G.H., Bouligand, C., Glen, J.M.G., Earney, T.E., Zielinski, L.A., Anderson, J.E., Kelly, P.J.: Development of small uncrewed aerial systems for multi-instrument geophysical data acquisition in active geothermal systems, Society of Exploration Geophysicists, Summit on Drone Geophysics, (2023), 50.

Roberts, C.W., Kucks, R.P., and Hill, P.L.: Oregon magnetic and gravity maps and data–A website for distribution of data, U.S. Geological Survey Data Series, (2008), DS-355.

Seequent, Oasis Montaj, 2022.2, (2022).

Travis, P.: Geology of the area near the north end of Summer Lake, Lake County, Oregon, Masters Thesis, University of Oregon, Eugene, Oregon, (1977), 95.

U.S. Geological Survey: 3D elevation program 10-meter resolution digital elevation model, accessed March 11, 2022 at URL https://www.usgs.gov/the-national-map-data-delivery.

U.S. Geological Survey: Quaternary fault and fold database for the United States, accessed April 18, 2022, at: https://www.usgs.gov/natural-hazards/earthquake-hazards/faults.

Walker, G.W.: Reconnaissance geologic map of the east half of the Klamath Falls (AMS) Quadrangle, Lake and Klamath counties, Oregon, U.S. Geological Survey Map, MF-260, (1963).

Walker, G.W., Peterson, N.V., and Greene, R.C.: Reconnaissance geologic map of the east half of the Crescent (AMS) Quadrangle, Lake, Deschutes and Crook countries, Oregon, U.S. Geological Survey Map, I-493, (1967).

Wells, R.E.: The geology of the Drake Peak Rhyolite Complex and the surrounding area, Lake County, Oregon, Masters Thesis, University of Oregon, Eugene, Oregon, (1975), 92.

Williams, T., Snyder, N., Gosnold, W.: Low-temperature projects of the Department of Energy's Geothermal Technologies Program: Evaluation and lessons learned, Proceedings, Geothermal Resources Council Transactions, Reno, NV, (2016).